Accepted Manuscript

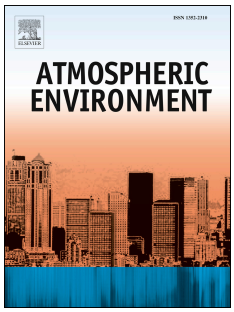

Vapor pressure predictions of multi-functional oxygen-containing organic compounds with COSMO-RS

Bernd Schröder, Michal Fulem, Mónia A.R. Martins

PII: S1352-2310(16)30206-0

DOI: 10.1016/j.atmosenv.2016.03.036

Reference: AEA 14518

To appear in: *Atmospheric Environment*

Received Date: 22 August 2015

Revised Date: 11 March 2016

Accepted Date: 14 March 2016

Please cite this article as: Schröder, B., Fulem, M., Martins, M.A.R., Vapor pressure predictions of multi-functional oxygen-containing organic compounds with COSMO-RS, *Atmospheric Environment* (2016), doi: 10.1016/j.atmosenv.2016.03.036.

Vapor pressure predictions of multi-functional oxygen-containing organic compounds with COSMO-RS

Bernd Schröder*[1], Michal Fulem[2], Mónia A. R. Martins[1]

1 Department of Chemistry, University of Aveiro, 3810-193 Aveiro, Portugal

2 Department of Physical Chemistry, University of Chemistry and Technology, Prague, Technická 5, 166 28, Prague 6, Czech Republic

*e-mail: bschroder@ua.pt

Abstract

Given the recent interest in multi-functional oxygen-containing organic compounds and the need of accurate and consistent data, a complete review and systematic analysis of available experimental vapor pressure data, as published in the original work of (Asher et al., 2002), was performed with the ThermoData Engine (TDE). A revised set of critical evaluated vapor pressure data, including their uncertainties based on the principles of dynamic data evaluation, is here recommended for a total of 58 compounds. COSMO-RS was further used for vapor pressure estimations for these compounds. The quality of the results is discussed in terms of the chemical functionalities of the molecules. To illustrate the partition behaviour of the title compounds under ambient conditions, a simple comparison of volatility binning between estimates and measurements was performed. Since the encountered vapor pressures are rather high, with respect to pressure range of semi-volatile organic compounds (SVOC), a large fraction is expected to stay in the atmosphere rather than to form secondary organic aerosol.

Keywords:

ThermoData Engine, Data evaluation, COSMO-RS, Vapor pressure prediction, Oxygenated compounds, Semi-volatile organic compounds

1. Introduction

The knowledge of organic aerosol (OA) formation is important for the understanding of certain aspects of climate change and for human health issues (Fuzzi et al., 2006). The gas/particle partitioning process of a given organic compound i in the atmosphere depends on its (sub-cooled) liquid vapor pressure, p_{iL}: if it decreases, the extent of the partitioning to a particulate material (PM) phase increases. When volatile organic compounds (VOCs) are oxidized, a variety of different oxygen-containing compounds covering an intermediate-to-low volatility range is formed. These compounds have an increased number of functionalities compared to their respective parent VOC compounds and, due to the resulting lower volatilities, may condense to form a secondary organic aerosol (SOA). Partitioning to the PM phase tends to increase with decreasing p_{iL}. The amount of SOA condensing in this process is quantifiable when applying gas/liquid equilibrium partitioning models using p_{iL} as the most important model input (Pankow, 1994). Correct vapor pressure data is hence a key parameter in the characterization of partitioning patterns of biogenic SOA, which is estimated to be a major contributor to organic aerosol (Hallquist et al., 2009), considering, for instance, SOA formed in oxidation processes altering ubiquitously occurring molecules in nature, such as isoprenes or terpenes. Few reliable literature vapor pressure data are commonly found for compounds with oxygenated functionalities and p_{iL} values down to (10^{-5} - 10^{-7}) kPa which roughly illustrates the range of potential formation of SOA products of interest. On the other hand, highly volatile compounds (p_L > 0.01 kPa) are not expected to be significantly present in the SOA phase. As a rule of thumb, to meet the requirement of sufficiently low (subcooled) vapor pressures for SOA formation, parent VOC compounds are equipped with six or more carbon atoms (Pankow et al., 2001). Low (sub-cooled) liquid vapor pressures, as frequently encountered at ambient temperatures, are difficult to measure (Růžička et al., 2012). Usually, data are of differing quality or not readily available for many low-volatility compounds that are of interest in research on atmospheric processes (Barley and McFiggans, 2010).

As experimental determinations can never keep pace with the data demand, a reliable and robust methodology for the prediction of vapor pressures for low-volatility compound is highly desirable (Capouet and Müller, 2006). Performance evaluation on available vapor pressure prediction methods is helpful in its concise choice with respect to a suitable volatility range and additional data requirements, e.g. (Compernolle et al., 2010). In a systematic approach, (Asher et al., 2002), (Asher and Pankow, 2006), as well as (Pankow and Asher, 2008) developed a UNIFAC-based group contribution method for the prediction of (sub-cooled) liquid vapor pressures, extending the work of (Jensen et al., 1981). This approach assumes that a given compound can be split into constituent groups, and that the (sub-cooled) liquid vapor pressure is determined by group-group interaction parameters. These interaction parameters can be obtained by training the method on a basis set of structurally related compounds with accurately known (sub-cooled) liquid vapor pressure data and the prerequisite of equilibrated basis and test sets. In general, these highly parameterized models give good results, but intrinsically, they are not able to differentiate between differences of certain isomers. In some cases, data for more exotic compounds maybe sought after (e.g., cyclic carbonyl containing compounds in SOA formed during ozone oxidation of common monoterpenes). Hence, besides accurate experimental determinations, reliable and (on a molecular level) versatile prediction methods are of utmost interest. With more and more new vapor pressure data on low-volatile organic substances becoming available, updated and new estimation methods appear (e.g., (Barley and McFiggans, 2010; Compernolle et al., 2011; Maadani et al., 2015; O'Meara et al., 2014)).

Traditional methods for correlating or predicting thermodynamic properties are primarily based on dividing the molecules into various groups (group-contribution methods - GCMs). COSMO-RS, the conductor-like screening model for realistic solvation, follows a different approach while combining quantum chemistry, dielectric continuum models, electrostatics surface interactions and statistical thermodynamics and can predict thermodynamic properties of neutral and charged molecules in the liquid phase. The method is based on a very small number of adjustable parameters, which are completely independent of any molecular or structural information (Klamt, 2005).

The work of (Asher et al., 2002) on the title compounds comprised 43 compounds in the basis set and 33 compounds in the test set. The main objectives of this work are two-fold: to establish a consistent set of vapor pressure data of multi-functional oxygen-containing organic compounds at ambient temperatures using the NIST ThermoData Engine (TDE), starting from the fore-mentioned work. Furthermore, the vapor pressure prediction capability of COSMO-RS on the title compounds against this newly created database of reliable vapor pressure data is evaluated, considering the quantum chemical BP-TZVP and BP-TZVPD-FINE levels of theory, setting-up vapor pressure estimations with the most stable individual conformer as well as with respective sets of the most relevant conformers.

2. Methods

2.1 The reference data set of critically evaluated experimental vapor pressures

Establishing a consistent reliable data base of experimentally based vapor pressure data is key to the success of development and verification of predictive models. In this work, the vapor pressure data used by Asher et al. were revised with the aid of the NIST ThermoData Engine 103b (TDE), which provides recommended critically evaluated thermodynamic data including their uncertainties based on the principles of dynamic data evaluation (Frenkel, 2005; Frenkel et al., 2005). In the enforcement of thermodynamic consistency of vapor pressure data, the following concepts are included in TDE i) ensuring the consistency of vapor pressure data with heat capacity differences between the liquid and gas phases at low pressures (for details on this technique, see (Růžička and Majer, 1994; Růžička and Majer, 1996)), and ii) ensuring the consistency of phase boundary lines and thermophysical properties at the solid-liquid-gas triple points T_{tp} (i.e. the liquid-vapor and solid-vapor curves must converge to the same triple-point pressure and the difference between the enthalpies of sublimation and vaporization derived from the vapor pressure equations at T_{tp} must yield the enthalpy of fusion).

A distinguishing feature of the TDE is that recommended data include estimates of uncertainties which are obtained as part of the dynamic critical evaluation based on partial uncertainties estimated at NIST for each experimental data point. Uncertainties developed by TDE represent estimates of the combined expanded uncertainty (level of confidence 0.95) for the property value, as defined in (Chirico et al., 2003). More

details about foundations of TDE, enforcement of thermodynamic consistency, and uncertainty evaluation can be found in (Frenkel et al., 2005).

The compounds gathered in Asher's data set from 2002 exert relatively high vapor pressures at ambient conditions, in almost all the cases, hence the assessment of this work is not regarding compounds with a high condensable fraction under ambient conditions.

2.2 COSMO-RS

In our work, we utilized the built-in vapor pressure estimation capability of COSMO-RS in its COSMOtherm implementation (Eckert and Klamt, 2014; Nakajoh et al., 2009; Schröder et al., 2010) on the same compounds as (Asher et al., 2002) did with their model (UNIFAC- p_L^o .1).

Extending the prediction of the chemical potential of liquids, COSMO-RS provides an *a priori* estimate of a pure compound's chemical potential in the gas phase, as described in eq.1:

$$\mu_i^{Gas} = E_i^{Gas} - E_i^{COSMO} - \omega^{Ring} n_i^{Ring} + \eta_{Gas} \qquad \text{(eq. 1)}$$

where E_i^{Gas} and E_i^{COSMO} are the total energies of the molecule in the gas phase and in the COSMO conductor, as obtained from quantum chemical calculations. The remaining contributions consist of the following terms: the correction for ring shaped molecules with n_i^{Ring} being the number of ring atoms in the molecule and ω^{Ring} an adjustable parameter, as well as η_{Gas}, providing the link between the reference states of the free energy of the compound in its gas and liquid state.

The vapor pressure of compound i is predicted via

$$p_{iL} = \exp\left[-\left(\mu_i^{Gas} - \mu_i^{i}\right) / RT\right] \qquad \text{(eq. 2)}$$

with R as the universal gas constant, μ_i^{Gas} as the chemical potential of the pure compound in the gas phase and μ_i^{i} as the chemical potential of the pure compound in itself (Eckert and Klamt, 2014).

Prior to any COSMO-RS calculation, to obtain the respective COSMO files, quantum-chemical optimizations were performed for all molecules in the gas phase as

well as in the COSMO state, using TURBOMOLE TmoleX v.4.0.1 (Steffen et al., 2010; TURBOMOLE, 2007-2014). To generate all relevant sets of conformers, COSMOconfX v.3.0 (COSMOconfX, 2013) was utilized. All optimizations were performed at the BP-TZVP as well as the new BP-TZVPD-FINE level of theory. In order to assure that a true minimum was reached, the encountered global gas phase minimum was subjected to vibrational frequency calculations with AOFORCE, in order to exclude the appearance of imaginary frequencies, at the respective BP-TZVP level of theory. Finally, vapor pressures were estimated at both levels of theory, applying COSMO-RS/ COSMOtherm's vapor pressure prediction feature, using the parameter file BP_TZVP_C30_1401.ctd (for COSMO files created at the BP-TZVP level of theory) and BP_TZVPD_FINE_C30_1401.ctd (for COSMO files created at the quantum chemical level BP-TZVPD-FINE, with a novel hydrogen bond interaction term and a novel van der Waals dispersion term) (Eckert, 2014).

3. Results and Discussion

3.1. Providing consistent data sets with TDE

To have the most correct base to compare estimations with available literature data in the given temperature range, the latter were re-examined. The critically assessed reference liquid vapor pressure data are given as parameter of the Wagner equation, Eq. 3, in Table 1, and evaluated at T = 298.15 K, including the combined expanded uncertainties in Table 2. In the case of compounds where TDE could not supply reference data, a search of the literature was conducted as well, but for the compounds in question, to our best of knowledge, no additional data were found. For the reason of comparison, Table 2 also contains COSMO-RS vapor pressure results regarding the BP-TZVPD-FINE basis set and all relevant conformers in the calculation, are given as well. SUPPLEMENTARY MATERIAL SM 4 presents the plot of COSMO-RS predictions from the BP-TZVPD-FINE method, regarding all relevant conformers, versus critically evaluated (subcooled) liquid vapor pressures, p_L, at T = 298.15 K.

The experimental data used to derive the parameters of the Wagner equation along with the references to the primary literature sources reporting these measurements are listed in Table "SM_experimental_data" as given in SUPPLEMENTARY DATA (SM).

********** **Table 1 near here**********

196 ********** **Table 2 near here**********

197 The evaluated vapor pressures are given as parameter of the Wagner equation, eq.3:

198 $\ln(p/p^o) - \ln(p_c/p^o) = T_c/T\,(A_1\cdot\tau + A_2\cdot\tau^{1.5} + A_3\cdot\tau^{2.5} + A_4\cdot\tau^5)$ (eq.3)

199 where $\tau = 1 - T/Tc$, with p_C the critical pressure, T_C the critical temperature and $p^o = 1$
200 kPa.

201 From the original basis set data of (Asher et al., 2002), Cyclobutanol, 3-Hydroxy-4-
202 methyl-2-pentanone, 2,4-Hexanedione, 2-Oxo-propanoic acid, Cyclopentanoic acid,
203 and Hexanedioic acid were excluded. For the first five compounds, no reliable vapor
204 pressure data besides data mainly predicted by the Ambrose-Walton method were
205 encountered in TDE, while for the latter, missing reliable phase transition data
206 impeded a meaningful estimation of subcooled liquid vapor pressure data. From the
207 original test set of Asher et al., 2,3-Pentandediol, 2,3-Dimethyl-2,3-butanediol, 2,4-
208 Dimethyl-cyclopentanol, 4-Hydroxy-2-pentanone, 5-Methyl-2-hexanone,
209 Cyclobutanoic acid, and Cyclohexanoic acid were excluded, due to missing reliable
210 TDE data, with sporadic data points far away from ambient temperature range,
211 complemented further only with predictions by the Ambrose-Walton method.

212 2-Acetylcyclopentanone, 2-Hydroxy-2-methyl-3-hexanone, Pinonaldehyde,
213 Caronaldehyde, 2-Hydroxypropanoic acid were also excluded: in theses cases, no data
214 were found at all.

215 Several compounds needed adjustments to obtain subcooled liquid vapor pressures in
216 the temperature range of interest, whether by recalculating p_L from p_S (a) or by
217 extrapolating from the Wagner equation (b).

218

219 This set of compounds subject to this treatment is comprised of 2,2,3,3-
220 Tetramethylbutane (a), Cyclohexanol (b), Pentanedioic acid (a), 2,2-Dimethyl-1-
221 propanol (a), 1,6-Hexanediol (b) and 4-Oxo-pentanoic acid (b).

222 For 2,2,3,3-Tetramethylbutane, subcooled liquid vapor pressure data was derived,
223 applying eq.5, which is derived from eq.4 (Allen et al., 1999):

224

$$\ln\left(\frac{p_{\mathrm{iL}}}{p_{\mathrm{iS}}}\right) = -\int_{T_{\mathrm{fus}}}^{T} \frac{\Delta_{\mathrm{s}}^{\mathrm{l}} H(T_{\mathrm{fus}}) + \int_{T_{\mathrm{fus}}}^{T} \Delta_{\mathrm{s}}^{\mathrm{l}} C_p(T)\, dT}{RT^2}\, dT \quad \text{(eq.4)}$$

$$\ln\left(\frac{p_{\mathrm{iL}}}{p_{\mathrm{iS}}}\right) = \frac{1}{RT}\left\{\frac{\Delta_{\mathrm{s}}^{\mathrm{l}} H(T_{\mathrm{fus}})}{T_{\mathrm{fus}}}(T_{\mathrm{fus}} - T) - (a_s - a_l)\left[T\ln(\frac{T_{\mathrm{fus}}}{T}) - (T_{\mathrm{fus}} - T)\right] + \frac{(b_s - b_l)}{2}(T_{\mathrm{fus}} - T)^2\right\}$$

(eq.5),

and using available phase transition literature data (refer to SUPPLEMENTARY MATERIAL SM1) for the melting point, T_{fus}, molar enthalpy of fusion, $\Delta_{\mathrm{s}}^{\mathrm{l}} H(T_{\mathrm{fus}})$, as well as the parameter for the nearly linear functions of heat capacities from temperature, both for the solid ($C_{\mathrm{p}}(\mathrm{s}) = a_s + b_s T$) and liquid state ($C_{\mathrm{p}}(\mathrm{l}) = a_l + b_l T$). Solid vapor pressures were calculated from the *pV* expansion equation (eq.6) whose parameter were obtained from TDE (please refer to SUPPLEMENTARY MATERIAL SM2):

$$\ln(p/p^o) = a_1 + a_2/T + a_3 \cdot \ln(T) + a_4 \cdot T + a_5 \cdot T^2 + a_6/T^2 + a_7 \cdot T^6 + a_8/T^4, \quad \text{(eq.6)}$$

where p^o = 1 kPa.

SUPPLEMENTARY MATERIAL SM 3 provides critically evaluated solid and liquid vapor pressures, p_{S} and p_{L}, at T = 298.15 K, for the compounds treated with equation 5.

The data for Cyclohexanol were extrapolated down to T = 290 K, given the limit of available experimental data for liquid vapor pressures being very close (T = 299.084 K). Deriving data for Pentanedioic acid applying eq. 5 is possible when accepting that there are no vapor pressure data related to the additional solid modification existing below T = 338 K, but that the corresponding heat capacities of the respective modifications above and below T = 338 K have nearly the same slope with temperature. Due to the availability of all necessary phase transition data according to eq.5, subcooled vapor pressure data were derived for 2,2-Dimethyl-1-propanol. For 1,6-Hexanediol, no data on the phase boundary pressure for the phase transition from crystal to gas were encountered; due to the proximity of the limit of available experimental data for liquid vapor pressures (T = 314.96 K), vapor pressures at the

target temperature range were obtained by extrapolation of the Wagner equation. A calculation of subcooled vapor pressures of 2,3-Dimethyl-2,3-butanediol in the targeted temperature range was not performed. A complete set of phase transition data according to eq.5 is not available. Furthermore, while the melting point is with T_{fus} = 316 K rather close to the wanted temperature range, reliable experimental liquid vapor pressure data were only recorded starting from T = 379.125 K. Hence, the compound was removed from the original test set of (Asher et al., 2002). Due to the incomplete sets of available phase transition data corresponding to the data requirements of eq.5 and the proximity of the limit of available experimental data, (subcooled) liquid vapor pressures of 4-Oxo-pentanoic acid (experimental data start at T = 306.1 K) were obtained through extrapolation from liquid vapor pressures.

3.2. Vapor pressure prediction with COSMO-RS

To evaluate the vapor pressure prediction capability of COSMO-RS on the title compounds against the newly created database of reliable vapor pressure data, the remaining compounds of Asher's original basis and test sets were combined to a set of 66 compounds. After generating all necessary COSMO files, vapor pressures were calculated in the temperature range of $290 \leq \langle T \rangle \leq 320$ K, at the same temperatures in the interval as considered by Asher et al. (2002), for the following input scenarios:

I) the most stable conformer, at the quantum chemical BP-TZVP level

II) the most stable conformer, at the quantum chemical BP-TZVPD-FINE level

III) a set of the most relevant conformers, at the quantum chemical BP-TZVP level

IV) a set of the most relevant conformers, at the quantum chemical BP-TZVPD-FINE level

In individual calculations, COSMO-RS provides the respective parameter for the Antoine equation, eq.7, as output:

$$\ln(p_{iL}) = A - B / (T + C) \qquad \text{(eq.7)}$$

To test the *a priori* predictive power of COSMO-RS, no experimental boiling points nor (p,T) data pairs were used as reference points for scaling the vapor pressure prediction outputs, which is optional in the COSMOtherm implementation designed

to clearly improve the results, given the availability of such high-quality experimental data. While most of the substances comprising aerosols do not have this information available, the approach is further justified due to the capability of COSMO-RS to excellently describe the temperature dependence of vapor pressures even for rather challenging low vapor pressure substances like ionic liquids (Schröder and Coutinho, 2014). All Antoine parameters, as obtained with COSMO-RS with respect to full conformer sets as well as the most stable conformers only, for both levels of theory examined (BP-TZVP and BP-TZVPD-FINE), are tabulated in the SUPPLEMENTARY DATA SM5. The agreement between experimental and predicted data and performance of prediction was evaluated with the standard error of the fit (eq.8) and the signed standard error of the fit (eq.9):

$$\sigma_{\mathrm{FIT}} = \frac{1}{N_{\mathrm{T}}}\frac{1}{N_{\mathrm{C}}}\sum_{\mathrm{i}=1}^{N_{\mathrm{C}}}\sum_{\mathrm{j}=1}^{N_{\mathrm{T}}}\left|\log p_{\mathrm{iL}}(T_{\mathrm{j}})_{\mathrm{E}} - \log p_{\mathrm{iL}}(T_{\mathrm{j}})_{\mathrm{P}}\right| \qquad \text{(eq.8)}$$

$$\sigma_{\mathrm{FIT,signed}} = \frac{1}{N_{\mathrm{T}}}\frac{1}{N_{\mathrm{C}}}\sum_{\mathrm{i}=1}^{N_{\mathrm{C}}}\sum_{\mathrm{j}=1}^{N_{\mathrm{T}}}\left[\log p_{\mathrm{iL}}(T_{\mathrm{j}})_{\mathrm{E}} - \log p_{\mathrm{iL}}(T_{\mathrm{j}})_{\mathrm{P}}\right] \qquad \text{(eq.9)}$$

with number of temperature points, N_{T}, number of compounds in the set, N_{C}, vapor pressures, p_{iL}, at temperatures T, experimental (suffix E) and predicted (suffix P). The main findings from statistical analysis are summarized in Table 3. Figures 1-4 are plots of the results for both COSMO-RS level of theories applied, concerning all relevant conformers. The plots related to the results of the most stable conformers are given as SUPPLEMENTARY DATA SM 6a-d.

********** **Table 3 near here**********

********** **Figures 1-4 near here**********

For the set of all compounds, as presented in Table 1, overall standard errors of the fit of σ_{FIT} = 0.301 log units (BP-TZVP) and σ_{FIT} = 0.285 log units (BP-TZVPD-FINE), for the full conformer sets, are obtained, which corresponds to a vapor pressure prediction to within a factor of about 2. The signed standard errors of the fit highlight an overestimation of vapor pressures. The values for both the standard errors of the fit and the signed standard errors of the fit shows that using a set of all relevant conformers gives better results, when compared with predictions applying only the most stable conformer. Analyzing the results by chemical functionalities, the best

results are obtained for aldehydes and ketones, e.g. predictions at the BP-TZVPD-FINE level of theory, for full conformer sets, result in almost not biased vapor pressure data to within a factor of 1.5. Performing the same predictions with the most stable conformer only will slightly increase the bias. Vapor pressures of carboxylic acids are generally overestimated in all applied modes, to within a factor of 3.

It needs to be taken into account that overestimation of vapor pressures of low-volatile substances is a serious issue to be kept in mind when the data should be further used to model SOA, as higher vapor pressures will result in a lesser amount of compound partitioning into the PM phase. The vapor pressures of the title compounds are rather high though, with respect to pressure ranges usually encountered for semi-volatile organic compounds (SVOC). A large fraction is expected to stay in the atmosphere rather than to form secondary organic aerosol. To roughly evaluate this effect on partitioning of semi-volatile organic compounds, the volatility binning principle of (Donahue et al., 2006) was applied.

With the assumption of a typical OA amount in moderately polluted ambient conditions of about 10 μg m^{-3}, the formation of OA was related to the volatility of the condensing species via its saturated vapor density obtained from eq. 10:

$$C_i^* = \frac{10^6 M_i \gamma_i p_{iL}}{RT} \qquad \text{(eq. 10)}$$

where M_i is the molecular weight, p_{iL} the saturated (subcooled) liquid vapor pressure of component I, while the activity coeffient γ_i is assumed to be unity.

The resulting C_i^* data (in μg m^{-3}) was transformed in its logarithmic form and accordingly binned, as proposed by (Donahue et al., 2006). Assuming the formation of 10 μg m^{-3} of OA, bin 1 represents equal partition (log C_i^* = 1 or C_i^* = 10 μg m^{-3}). Bin 2 compounds remain largely in the gaseous phase, while bin 0 compounds mainly condense; other bins might be added. This procedure was applied to those compounds for which reliable (subcooled) liquid vapor pressures could be established, at T = 298.15 K, as well as for the respective COSMO-RS data, at the BP-TZVPD-FINE level of theory. The results are given as SUPPLEMENTARY DATA SM7. To have considerable levels of condensation to form second organic aerosol, compounds with vapor pressures below 10^{-2} Pa are of utter relevance. Recent vapor pressure estimation

methodology is concerned addressing this issue by increasing the number of relevant compounds while shifting the vapor pressure range of test set data downwards (e.g. O'Meara et al. 2014, average vapor pressure of 90 compounds in the test set is 2.7 Pa at T = 298.15 K). With an average vapor pressure of 2.15 kPa, at T = 298.15 K, the vapor pressures of the examined 58 compounds of this work are in general too high to result in an appreciable condensation (only pentanedioic acid as a bin 2 compound is indicated in at least partially doing so, while the other compounds will remain in the gaseous phase), the effect of differing vapor pressure inputs is clearly illustrated by the method. While the vapor pressures of the examined compounds are in general too high to result in an appreciable condensation (only pentanedioic acid as a bin 2 compound is indicated in at least partially doing so, while the other compounds will remain in the gaseous phase), the effect of differing vapor pressure inputs is clearly illustrated by the method. The overall performance of COSMO-RS is good. Three compounds are sorted to the next lower bin, while eight compounds move to the next higher bin, with emphasis on carboxylic acids. A more pronounced case is 1,2,3-propanetriol: the overestimation of the vapor pressure in COSMO-RS leads to a change from bin 3 to bin 5, with respect to the experimentally established vapor pressure.

When comparing with vapor pressure estimations of other prediction methods applied to the set of title compounds, the overall performance of COSMO-RS is good and comparable with SPARC, taking into account that both programs were not trained on Asher's basis set (Asher et al., 2002). Unlike the results obtained with UNIFAC and SPARC, for which a separation into different functionalities still gives comparable errors, COSMO-RS shows a distinct spread in the quality of results. When compared with other methods, COSMO-RS yields best results for aldehydes and ketones (results with minimal bias), as depicted in SUPPLEMENTARY DATA 8. There, all data except the COSMO-RS data from this work were taken unadjusted from Asher's original work et al. (Asher et al., 2002). More recent vapor pressure estimation methods (e.g., Asher et al. 2008, Barley et al. 2010, Compernolle et al. 2011, O'Meara et al. 2014) are focused on substances with potential of SOA formation. They generally try to address compounds of lower vapor pressure ranges, with, at times, a wide variability on available data, as well as in their chemistries - some of them rather exotic. Less common substances such as organic hydroperoxides, peroxy acyl nitrates

or peracids are introducing issues with respect to a compound's thermal stability and purity and hence, turn the measurements of their vapor pressures into a challenging task. But even for supposedly more simple compounds, all but agreement in available vapor pressure data may be encountered, as we have shown here. Given the importance of reliable vapor pressure data in establishing estimation methods, it is the primary goal of this work to establish some common ground, which is to be enlarged in our future work.

4. Conclusions

Trying to establish a consistent reliable data base of experimentally based vapor pressure data, at ambient conditions, clearly shows that even for the supposedly well known title compounds, problems rather frequently occur. This issue is expected to be even more aggravated for more complex compounds, preferentially in the low vapor pressure range. Albeit measuring all compounds is impossible, the chance given by the recent technological developments in high-accuracy vapor pressure measurements should be concisely embraced. It should be focused in measuring key compounds to be defined, and re-measuring other important compounds where available data are of dubious quality, even more so as these data are supposed to serve as the future's foundation of predictive routines. In this aspect, TDE is a powerful supporting tool.

Within the frame of this work, COSMO-RS was found to predict vapor pressures of the set of title compounds, in the temperature range of $290 \leq \langle T \rangle \leq 320$ K, to within a factor of 2, but with a tendency to overestimate data, predominantly for carboxylic acids, and working best for aldehydes and ketones.

Our future work is focused on the extension of the approach to unsaturated and aromatic compounds, further accompanied by a continued critical generation of new reference data. Research on SOA formation and composition is identifying more and more semi-volatile or non-volatile compounds of interest, for which no reliable experimental physico-chemical data are available, nor group contribution methods could be fully applied, yet, e.g. compounds discovered in ozonolysis reactions of terpenes (Jenkin, 2004). The application of COSMO-RS, with its approach to derive physico-chemical properties from pairwise-interacting surfaces only, could provide an advantageous alternative in such cases.

5. References

Allen, J.O., Sarofim, A.F., Smith, K.A., 1999. Thermodynamic Properties of Polycyclic Aromatic Hydrocarbons in the Subcooled Liquid State. Polycyclic Aromatic Compounds 13, 261-283.

Asher, W.E., Pankow, J.F., 2006. Vapor pressure prediction for alkenoic and aromatic organic compounds by a UNIFAC-based group contribution method. Atmospheric Environment 40, 3588-3600.

Asher, W.E., Pankow, J.F., Erdakos, G.B., Seinfeld, J.H., 2002. Estimating the vapor pressures of multi-functional oxygen-containing organic compounds using group contribution methods. Atmospheric Environment 36, 1483-1498.

Barley, M.H., McFiggans, G., 2010. The critical assessment of vapour pressure estimation methods for use in modelling the formation of atmospheric organic aerosol. Atmos. Chem. Phys. 10, 749-767.

Capouet, M., Müller, J.F., 2006. A group contribution method for estimating the vapour pressures of α-pinene oxidation products. Atmos. Chem. Phys. 6, 1455-1467.

Compernolle, S., Ceulemans, K., Müller, J.F., 2010. Technical Note: Vapor pressure estimation methods applied to secondary organic aerosol constituents from α-pinene oxidation: an intercomparison study. Atmos. Chem. Phys. 10, 6271-6282.

Compernolle, S., Ceulemans, K., Müller, J.F., 2011. EVAPORATION: a new vapour pressure estimation methodfor organic molecules including non-additivity and intramolecular interactions. Atmos. Chem. Phys. 11, 9431-9450.

COSMOconfX, 2013. COSMOconfX v3.0. COSMOlogic. GmbH & Co. , Leverkusen.

Donahue, N.M., Robinson, A.L., Stanier, C.O., Pandis, S.N., 2006. Coupled Partitioning, Dilution, and Chemical Aging of Semivolatile Organics. Environ. Sci. Technol. 40, 2635-2643.

Eckert, F., 2014. COSMOtherm Reference Material, Version C3.0 Release 14.01. COSMOlogic. GmbH & Co. , Leverkusen.

Eckert, F., Klamt, A., 2014. COSMOtherm. Version C3.0 Release 14.01. COSMOlogic, GmbH & Co. Kg, Leverkusen.

Frenkel, M., 2005. Global communications and expert systems in thermodynamics: Connecting property measurement and chemical process design. Pure Appl. Chem. 77.

Frenkel, M., Chirico, R.D., Diky, V., Yan, X., Dong, Q., Muzny, C., 2005. ThermoData Engine (TDE): Software Implementation of the Dynamic Data Evaluation Concept. Journal of Chemical Information and Modeling 45, 816-838.

Fuzzi, S., Andreae, M.O., Huebert, B.J., Kulmala, M., Bond, T.C., Boy, M., Doherty, S.J., Guenther, A., Kanakidou, M., Kawamura, K., Kerminen, V.M., Lohmann, U.,

Russell, L.M., Pöschl, U., 2006. Critical assessment of the current state of scientific knowledge, terminology, and research needs concerning the role of organic aerosols in the atmosphere, climate, and global change. Atmos. Chem. Phys. 6, 2017-2038.

Hallquist, M., Wenger, J.C., Baltensperger, U., Rudich, Y., Simpson, D., Claeys, M., Dommen, J., Donahue, N.M., George, C., Goldstein, A.H., Hamilton, J.F., Herrmann, H., Hoffmann, T., Iinuma, Y., Jang, M., Jenkin, M.E., Jimenez, J.L., Kiendler-Scharr, A., Maenhaut, W., McFiggans, G., Mentel, T.F., Monod, A., Prévôt, A.S.H., Seinfeld, J.H., Surratt, J.D., Szmigielski, R., Wildt, J., 2009. The formation, properties and impact of secondary organic aerosol: current and emerging issues. Atmos. Chem. Phys. 9, 5155-5236.

Chirico, R.D., Frenkel, M., Diky, V.V., Marsh, K.N., Wilhoit, R.C., 2003. ThermoMLAn XML-Based Approach for Storage and Exchange of Experimental and Critically Evaluated Thermophysical and Thermochemical Property Data. 2. Uncertainties. J. Chem. Eng. Data 48, 1344-1359.

Jenkin, M.E., 2004. Modelling the formation and composition of secondary organic aerosol from α- and β-pinene ozonolysis using MCM v3. Atmos. Chem. Phys. 4, 1741-1757.

Jensen, T., Fredenslund, A., Rasmussen, P., 1981. Pure-component vapor pressures using UNIFAC group contribution. Industrial & Engineering Chemistry Fundamentals 20, 239-246.

Klamt, A., 2005. COSMO-RS From Quantum Chemistry to Fluid PhaseThermodynamics and Drug Design. Elsevier, Amsterdam.

Maadani, H., Salahinejad, M., Ghasemi, J.B., 2015. Global and local QSPR models to predict supercooled vapour pressure for organic compounds. SAR QSAR Environ. Res. 26, 1033-1045.

Nakajoh, K., Grabda, M., Oleszek-Kudlak, S., Shibata, E., Eckert, F., Nakamura, T., 2009. Prediction of vapour pressures of chlorobenzenes and selected polychlorinated biphenyls using the COSMO-RS model. J. Mol. Struct.: THEOCHEM 895, 9-17.

O'Meara, S., Booth, A.M., Barley, M.H., Topping, D., McFiggans, G., 2014. An assessment of vapour pressure estimation methods. Phys. Chem. Chem. Phys. 16, 19453-19469.

Pankow, J.F., 1994. An absorption model of gas/particle partitioning of organic compounds in the atmosphere. Atmospheric Environment 28, 185-188.

Pankow, J.F., Asher, W.E., 2008. SIMPOL.1: a simple group contribution method for predicting vapor pressures and enthalpies of vaporization of multifunctional organic compounds. Atmos. Chem. Phys. 8, 2773-2796.

Pankow, J.F., Seinfeld, J.H., Asher, W.E., Erdakos, G.B., 2001. Modeling the Formation of Secondary Organic Aerosol. 1. Application of Theoretical Principles to Measurements Obtained in the α-Pinene/, β-Pinene/, Sabinene/, Δ3-Carene/, and Cyclohexene/Ozone Systems. Environ. Sci. Technol. 35, 1164-1172.

485 Růžička, K., Koutek, B., Fulem, M., Hoskovec, M., 2012. Indirect determination of
486 vapor pressures by capillary gas-liquid chromatography: Analysis of the reference
487 vapor-pressure data and their treatment. J. Chem. Eng. Data 57, 1349−1368.

488 Růžička, K., Majer, V., 1994. Simultaneous treatment of vapor pressures and related
489 thermal data between the triple and normal boiling temperatures for *n*-alkanes C_5-C_{20}.
490 J. Phys. Chem. Ref. Data 23, 1-39.

491 Růžička, K., Majer, V., 1996. Simple and controlled extrapolation of vapor pressures
492 toward the triple point. AIChE J. 42, 1723-1740.

493 Schröder, B., Coutinho, J.A.P., 2014. Predicting enthalpies of vaporization of aprotic
494 ionic liquids with COSMO-RS. Fluid Phase Equilib. 370, 24-33.

495 Schröder, B., Santos, L.M.N.B.F., Rocha, M.A.A., Oliveira, M.B., Marrucho, I.M.,
496 Coutinho, J.A.P., 2010. Prediction of environmental parameters of polycyclic
497 aromatic hydrocarbons with COSMO-RS. Chemosphere 79, 821-829.

498 Steffen, C., Thomas, K., Huniar, U., Hellweg, A., Rubner, O., Schroer, A., 2010.
499 TmoleX—A graphical user interface for TURBOMOLE. J. Comput. Chem. 31, 2967-
500 2970.

501 TURBOMOLE, 2007-2014. A development of University of Karlsruhe and
502 Forschungszentrum Karlsruhe GmbH, 1989-2013, TURBOMOLE GmbH, 2007-
503 2014; http://www.turbomole.com/.

504

505 ***Acknowledgments:***

506 This work was financed by national funding from FCT (Fundação para a Ciência e a
507 Tecnologia) through the project PTDC/AAC-AMB/121161/2010, by FEDER
508 fundings through program COMPETE and by national fundings through FCT in the
509 ambit of project CICECO - FCOMP-01-0124-FEDER-037271 (Ref. FCT Pest-
510 C/CTM/LA0011/2013). Mónia Martins is grateful to Fundação Para a Ciência e
511 Técnologia, Lisboa, Portugal, and the European Social Fund (ESF) under the 3rd
512 Community Support Framework (CSF), for the award of a Post-Doc scholarship
513 (SFRH/BD/87084/2012).

514

515

516

517

518

1

2 ***TABLES***

3

4

Table 1. Critical evaluated experimental vapor pressure data. Parameter for the Wagner equation (eq.3).

.

Compound	Sum formula	Validity range/ K	T_c/ K	$\ln(p_c/p^o)$	A_1	A_2	A_3	A_4
Non-oxygenated hydrocarbons								
Cyclohexane	C6H12	279.816 to 553.403	553.403	8.31116	-7.03242	1.63322	-2.04012	-3.26885
1,1-Dimethylcyclopentane	C7H14	203.723 to 557	557	8.25961	-7.53903	2.28569	-2.24658	-3.36596
trans-1,3-Dimethylcyclopentane	C7H14	139.29 to 551	551	8.12578	-7.34339	1.68655	-2.11601	-3.06139
2,2-Dimethylpentane	C7H16	149.444 to 520.46	520.46	7.91496	-7.44988	1.90597	-2.79228	-2.65569
1,1-Dimethylcyclohexane	C8H16	239.837 to 598	598	8.15742	-7.74867	2.72954	-2.87454	-2.76804
cis-1,2-Dimethylcyclohexane	C8H16	223.318 to 605.6	605.6	8.08534	-7.37043	1.54767	-1.8956	-3.67185
2,2,4-Trimethylpentane	C8H18	165.786 to 543.909	543.909	7.851	-7.59422	1.91	-2.61495	-3.2085

2,3,4-Trimethylpentane	C8H18	163.81 to 566.373	566.373	7.9043	-7.5089	1.61984	-2.43858	-3.35281
2,2,3,3-Tetramethylbutane	C8H18	373.944 to 565	565	7.91145	-7.37629	1.98094	-2.50594	-2.19192
Alcohols								
1,2-Propanediol	C3H8O2	242.8 to 676.4	676.4	8.69045	-9.21309	3.54716	-8.08038	-1.32069
2-Butanol	C4H10O	184.712 to 535.95	535.95	8.35245	-9.0333	4.49341	-11.8265	3.35098
2-Methyl-1-propanol	C4H10O	171.193 to 548.443	548.443	8.36479	-7.91829	1.33988	-8.01794	0.746464
1-Butanol	C4H10O	184.552 to 561.961	561.961	8.38478	-8.49064	2.47834	-8.86072	1.62852
1,4-Butanediol	C4H10O2	293.575 to 724.255	724.255	8.64635	-12.1855	10.9737	-18.3372	8.37101
2,3-Butanediol	C4H10O2	190 to 633	633	8.60161	-16.4421	16.9449	-16.6489	-5.28866
1,3-Butanediol	C4H10O2	210 to 679.28	679.28	8.4612	-11.5558	7.99332	-13.5099	2.57618
1,2-Butanediol	C4H10O2	210 to 680	680	8.58726	-10.6917	6.73819	-11.0636	-0.927427
1,5-Pentanediol	C5H12O2	249.1 to 731	731	8.29423	-11.3817	10.5443	-19.0681	0.623831
1-Pentanol	C5H12O	195.571 to 588.033	588.033	8.27094	-8.85937	3.77873	-10.3926	1.72802
Cyclohexanol	C6H12O	299.084 to 647.1	647.1	8.36672	-10.4728	10.285	-16.3972	3.46667

1-Hexanol	C6H14O	226.7 to 610.399	610.399	8.13537	-9.41927	5.36679	-12.0371	1.40258
2-Methyl-2-pentanol	C6H14O	170 to 559.461	559.461	8.16991	-17.491	25.2286	-29.715	7.6794
2,3-Dimethyl-2-butanol	C6H14O	262.68 to 559	559	8.21548	-13.4235	15.1789	-20.7719	10.582
2-Methyl-2,4-pentanediol	C6H14O2	200 to 657	657	8.13966	-9.87598	5.26051	-12.3373	3.49066
2-Methyl-cis-cyclohexanol	C7H14O	220 to 637	637	8.31509	-13.0149	13.5592	-16.1385	0.195312
1,2,3-Propanetriol	C3H8O3	290.83 to 850	850	8.92237	-11.0723	9.31962	-14.099	1.90561
2,2-Dimethyl-1-propanol	C5H12O	328.2 to 559.9	559.9	8.23098	-7.13175	0.447081	-5.83156	-9.75492
2-Pentanol	C5H12O2	134.18 to 560.315	560.315	8.20942	-9.98372	7.28506	-14.8256	4.01185
1,2-Pentanediol	C5H12O2	210 to 676	676	8.29981	-10.3	5.34532	-11.0345	-1.05818
3-Hexanol	C6H14O	180 to 582.437	582.437	8.10406	-18.1786	28.2342	-34.0766	11.0559
1,6-Hexanediol	C6H14O2	314.95 to 740.8	740.8	8.41522	-12.4552	10.8631	-17.1674	-1.40484
Cycloheptanol	C7H14O	280.299 to 668	668	8.26781	-12.0359	12.4959	-16.8113	1.05845
1,7-Heptanediol	C7H16O2	295 to 738	738	8.11827	-10.4583	3.77007	-7.74848	-4.97477

Aldehydes and ketones

Butanal	C4H8O	176.292 to 522.28	522.28	8.39187	-11.0676	8.75124	-7.86955	-0.680155
2-Methylpropanal	C4H8O	201.04 to 543.61	543.61	8.54039	-6.66191	1.81764	-3.7044	-
Cyclopentanone	C5H8O	221.449 to 624.459	624.459	8.42778	-7.12419	0.965934	-1.71592	-3.52205
Cyclohexanone	C6H10O	245.216 to 664.9	664.9	8.39832	-7.36605	1.85019	-2.5712	-2.85463
3-Hexanone	C6H12O	217.71 to 583.082	583.082	8.10834	-7.98941	2.12035	-3.30657	-3.39445
4-Hydroxy-4-methyl-2-pentanone	C6H12O2	288.15 to 624	624	8.98504	-13.9654	6.57638	-	-
Heptanal	C7H14O	229.208 to 616.769	616.769	8.0607	-9.04924	4.05691	-4.68397	-3.59322
Hexanal	C6H12O	214.93 to 591.702	591.702	8.14694	-8.00278	2.1825	-4.06203	-2.29781
2-Heptanone	C7H14O	237.4 to 611.421	611.421	7.99923	-8.44973	2.79615	-4.29262	-3.15949
Octanal	C8H16O	247.73 to 639.3	639.3	7.99533	-9.89557	7.10889	-11.2161	5.26975
2-Octanone	C8H16O	252.841 to 632.7	632.7	7.90075	-8.81646	3.53191	-5.5287	-3.06412
Carboxylic acids								
Propanoic	C3H6O2	252.654 to 602.645	602.645	8.4219	-10.608	7.46932	-11.3394	5.90657
2-Methylpropanoic	C4H8O2	226.8 to 604.96	604.96	8.21602	-8.63096	1.67018	-5.93647	0.00221635

Butanoic	C4H8O2	268.031 to 621.585	621.585	8.28508	-9.998	5.66138	-11.132	6.11869
3-Methylbutanoic	C5H10O2	243.52 to 628.958	628.958	8.13105	-9.7391	4.8407	-11.1037	5.61955
Pentanedioic	C5H8O4	371 to 840	840	8.37636	-12.8883	9.05607	-11.3925	-4.26311
Ethanoic	C2H4O2	289.686 to 592.998	592.998	8.66314	-8.48411	1.4693	-0.60354	-6.05104
Pentanoic	C5H10O2	239.517 to 639.493	639.493	8.13406	-8.33573	0.501971	-5.88528	-0.876692
4-Oxo-pentanoic	C5H8O3	306.1 to 712	712	8.1662	-10.7327	4.00015	-8.30982	-5.06789
2-Ethyl-butanoic	C6H12O2	241.38 to 644	644	8.06234	-13.6977	14.7062	-21.4486	4.27431
4-Methyl-pentanoic	C6H12O2	200 to 640	640	8.07998	-14.1645	13.1666	-17.9421	1.91519
Hexanoic	C6H12O2	269.04 to 661.043	661.043	8.13782	-12.3373	10.5031	-16.9283	6.21067
Heptanoic	C7H14O2	265.98 to 678.484	678.484	8.0186	-9.62445	3.93377	-11.4601	3.69713
Octanoic	C8H16O2	289.656 to 693.71	693.71	7.95745	-14.517	16.2309	-24.6374	12.8228
Nonanoic	C9H18O2	285.527 to 711.941	711.94	7.76963	-9.43218	3.49435	-10.9878	-

Table 2. Critically evaluated reference liquid vapor pressures p_L, at T = 298.15 K. COSMO-RS predictions as obtained from the BP-TZVPD-FINE method, regarding all relevant conformers, are included as well.

Compound	p_L(reference)/kPa	U_c/kPa[a]	p_L(COSMO-RS, BP-TZVPD-FINE, all conformers)/kPa
Non-oxygenated hydrocarbons			
Cyclohexane	$1.30 \cdot 10^{1}$	$2.7 \cdot 10^{-2}$	$1.80 \cdot 10^{1}$
1,1-Dimethylcyclopentane	$1.01 \cdot 10^{1}$	$1.7 \cdot 10^{-1}$	$1.03 \cdot 10^{1}$
trans-1,3-Dimethylcyclopentane	$8.97 \cdot 10^{0}$	$7.2 \cdot 10^{-2}$	$9.14 \cdot 10^{0}$
2,2-Dimethylpentane	$1.40 \cdot 10^{1}$	$2.6 \cdot 10^{-2}$	$1.66 \cdot 10^{1}$
1,1-Dimethylcyclohexane	$3.02 \cdot 10^{0}$	$1.4 \cdot 10^{-1}$	$2.96 \cdot 10^{0}$
cis-1,2-Dimethylcyclohexane	$1.94 \cdot 10^{0}$	$1.0 \cdot 10^{-2}$	$2.75 \cdot 10^{0}$
2,2,4-Trimethylpentane	$6.58 \cdot 10^{0}$	$5.1 \cdot 10^{-2}$	$8.18 \cdot 10^{0}$
2,3,4-Trimethylpentane	$3.62 \cdot 10^{0}$	$1.3 \cdot 10^{-2}$	$7.29 \cdot 10^{0}$
2,2,3,3-Tetramethylbutane	$5.28 \cdot 10^{0}$	$9.0 \cdot 10^{-2}$	$9.28 \cdot 10^{0}$
Alcohols			
1,2-Propanediol	$1.69 \cdot 10^{-2}$	$3.0 \cdot 10^{-4}$	$1.80 \cdot 10^{-2}$
2-Butanol	$2.33 \cdot 10^{0}$	$1.0 \cdot 10^{-1}$	$1.22 \cdot 10^{0}$
2-Methyl-1-propanol	$1.54 \cdot 10^{0}$	$1.2 \cdot 10^{-2}$	$1.16 \cdot 10^{0}$
1-Butanol	$9.26 \cdot 10^{-1}$	$3.7 \cdot 10^{-2}$	$7.01 \cdot 10^{-1}$
1,4-Butanediol	$7.99 \cdot 10^{-4}$	$3.1 \cdot 10^{-5}$	$2.16 \cdot 10^{-3}$
2,3-Butanediol	$1.84 \cdot 10^{-2}$	$7.5 \cdot 10^{-3}$	$2.21 \cdot 10^{-2}$
1,3-Butanediol	$3.74 \cdot 10^{-3}$	$6.1 \cdot 10^{-5}$	$3.12 \cdot 10^{-3}$
1,2-Butanediol	$8.92 \cdot 10^{-3}$	$1.7 \cdot 10^{-4}$	$1.88 \cdot 10^{-2}$

1,5-Pentanediol	$1.29 \cdot 10^{-4}$	$5.8 \cdot 10^{-5}$	$2.82 \cdot 10^{-4}$
1-Pentanol	$3.13 \cdot 10^{-1}$	$2.6 \cdot 10^{-2}$	$2.01 \cdot 10^{-1}$
Cyclohexanol	$1.08 \cdot 10^{-1}$	$3.7 \cdot 10^{-3}$	$2.15 \cdot 10^{-1}$
1-Hexanol	$1.09 \cdot 10^{-1}$	$9.1 \cdot 10^{-3}$	$1.02 \cdot 10^{-1}$
2-Methyl-2-pentanol	$9.59 \cdot 10^{-1}$	$7.0 \cdot 10^{-2}$	$4.96 \cdot 10^{-1}$
2,3-Dimethyl-2-butanol	$1.21 \cdot 10^{0}$	$3.0 \cdot 10^{-2}$	$7.06 \cdot 10^{-1}$
2-Methyl-2,4-pentanediol	$9.21 \cdot 10^{-3}$	$4.9 \cdot 10^{-4}$	$1.16 \cdot 10^{-3}$
2-Methyl-cis-cyclohexanol	$9.68 \cdot 10^{-2}$	$2.2 \cdot 10^{-3}$	$9.13 \cdot 10^{-2}$
1,2,3-Propanetriol	$2.26 \cdot 10^{-5}$	$1.4 \cdot 10^{-6}$	$1.14 \cdot 10^{-3}$
2,2-Dimethyl-1-propanol	$1.28 \cdot 10^{0}$	$1.6 \cdot 10^{-1}$	$1.16 \cdot 10^{0}$
2-Pentanol	$8.26 \cdot 10^{-1}$	$1.6 \cdot 10^{-2}$	$4.72 \cdot 10^{-1}$
1,2-Pentanediol	$3.47 \cdot 10^{-3}$	$1.6 \cdot 10^{-4}$	$1.25 \cdot 10^{-2}$
3-Hexanol	$4.06 \cdot 10^{-1}$	$1.5 \cdot 10^{-2}$	$3.37 \cdot 10^{-1}$
1,6-Hexanediol	$4.94 \cdot 10^{-4}$	$1.7 \cdot 10^{-5}$	$8.33 \cdot 10^{-5}$
Cycloheptanol	$2.74 \cdot 10^{-2}$	$1.2 \cdot 10^{-3}$	$1.98 \cdot 10^{-2}$
1,7-Heptanediol	$1.01 \cdot 10^{-4}$	$6.0 \cdot 10^{-4}$	$2.79 \cdot 10^{-5}$
Aldehydes and ketones			
Butanal	$1.49 \cdot 10^{1}$	$4.3 \cdot 10^{-1}$	$2.10 \cdot 10^{1}$
2-Methylpropanal	$2.30 \cdot 10^{1}$	$4.0 \cdot 10^{-1}$	$2.94 \cdot 10^{1}$
Cyclopentanone	$1.49 \cdot 10^{0}$	$1.4 \cdot 10^{-2}$	$1.76 \cdot 10^{0}$
Cyclohexanone	$5.53 \cdot 10^{-1}$	$1.4 \cdot 10^{-2}$	$5.07 \cdot 10^{-1}$
3-Hexanone	$1.87 \cdot 10^{0}$	$8.0 \cdot 10^{-3}$	$1.66 \cdot 10^{0}$
4-Hydroxy-4-methyl-2-pentanone	$3.38 \cdot 10^{-1}$	$5.9 \cdot 10^{-2}$	$9.46 \cdot 10^{-2}$
Heptanal	$5.35 \cdot 10^{-1}$	$1.8 \cdot 10^{-1}$	$6.63 \cdot 10^{-1}$
Hexanal	$1.28 \cdot 10^{0}$	$1.2 \cdot 10^{-1}$	$2.17 \cdot 10^{0}$
2-Heptanone	$5.17 \cdot 10^{-1}$	$2.2 \cdot 10^{-3}$	$4.17 \cdot 10^{-1}$
Octanal	$1.50 \cdot 10^{-1}$	$6.0 \cdot 10^{-3}$	$2.13 \cdot 10^{-1}$

2-Octanone	$1.71 \cdot 10^{-1}$	$3.9 \cdot 10^{-2}$	$1.34 \cdot 10^{-1}$
Carboxylic acids			
Propanoic	$4.70 \cdot 10^{-1}$	$1.6 \cdot 10^{-2}$	$3.25 \cdot 10^{-1}$
2-Methylpropanoic	$1.93 \cdot 10^{-1}$	$6.4 \cdot 10^{-3}$	$4.15 \cdot 10^{-1}$
Butanoic	$1.13 \cdot 10^{-1}$	$5.6 \cdot 10^{-3}$	$2.98 \cdot 10^{-1}$
3-Methylbutanoic	$4.97 \cdot 10^{-2}$	$1.4 \cdot 10^{-3}$	$1.40 \cdot 10^{-1}$
Pentanedioic	$1.75 \cdot 10^{-6}$	$5.0 \cdot 10^{-7}$	$2.05 \cdot 10^{-6}$
Ethanoic	$2.06 \cdot 10^{0}$	$3.8 \cdot 10^{-2}$	$8.94 \cdot 10^{-1}$
Pentanoic	$2.48 \cdot 10^{-2}$	$1.9 \cdot 10^{-3}$	$9.52 \cdot 10^{-2}$
4-Oxo-pentanoic	$5.46 \cdot 10^{-4}$	$7.8 \cdot 10^{-4}$	$3.10 \cdot 10^{-4}$
2-Ethyl-butanoic	$9.05 \cdot 10^{-3}$	$3.6 \cdot 10^{-3}$	$1.11 \cdot 10^{-1}$
4-Methyl-pentanoic	$6.88 \cdot 10^{-3}$	$1.7 \cdot 10^{-3}$	$3.69 \cdot 10^{-2}$
Hexanoic	$6.09 \cdot 10^{-3}$	$3.1 \cdot 10^{-4}$	$2.35 \cdot 10^{-2}$
Heptanoic	$2.09 \cdot 10^{-3}$	$2.7 \cdot 10^{-4}$	$9.46 \cdot 10^{-3}$
Octanoic	$6.64 \cdot 10^{-4}$	$6.1 \cdot 10^{-5}$	$3.12 \cdot 10^{-3}$
Nonanoic	$2.29 \cdot 10^{-4}$	$1.0 \cdot 10^{-4}$	$1.09 \cdot 10^{-3}$

[a] U_c = Combined expanded uncertainty with 95 % level of confidence. The uncertainties listed are estimated as part of the dynamic critical evaluation by TDE.

Table 3. COSMO-RS results, as evaluated applying the standard error of the fit (eq.8) and the signed standard error of the fit (eq.9).

Compounds	N_C		COSMO-RS			
			all conformers		conf_c0	
			BP-TZVP	BP-TZVP-FINE	BP-TZVP	BP-TZVP-FINE
Hydocarbons	9	σ_{FIT}	0.163	0.115	0.163	0.115
		$\sigma_{FIT,signed}$	-0.125	-0.114	-0.125	-0.114
Alcoholes	24	σ_{FIT}	0.289	0.293	0.327	0.302
		$\sigma_{FIT,signed}$	-0.193	-0.124	-0.214	-0.018
Aldehydes	11	σ_{FIT}	0.192	0.144	0.178	0.132
		$\sigma_{FIT,signed}$	-0.088	0.008	-0.101	-0.004
Carboxylic acids	14	σ_{FIT}	0.498	0.491	0.511	0.518
		$\sigma_{FIT,signed}$	-0.410	-0.424	-0.443	-0.437

Total	58	σ_{FIT}	0.301	0.285	0.318	0.293
		$\sigma_{FIT,signed}$	-0.193	-0.124	-0.234	-0.131

FIGURES

FIGURE 1. Predicted COSMO-RS vapor pressures vs. critical evaluated experimental vapor pressures, at the BP-TZVP level of theory, full conformer sets (captions valid for all figures).

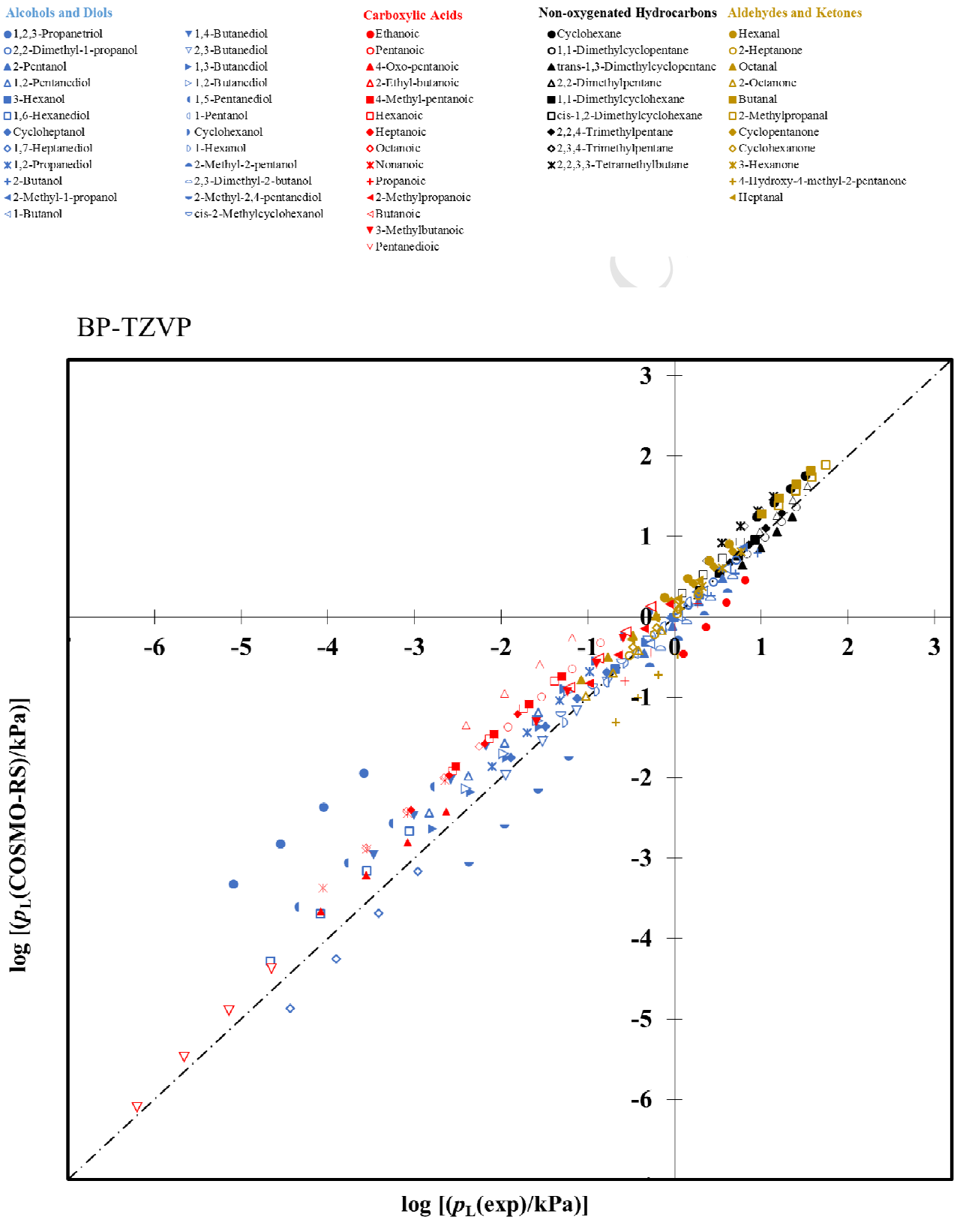

FIGURE 2. Predicted COSMO-RS vapor pressures vs. critical evaluated experimental vapor pressures, at the BP-TZVPD-FINE level of theory, full conformer sets.

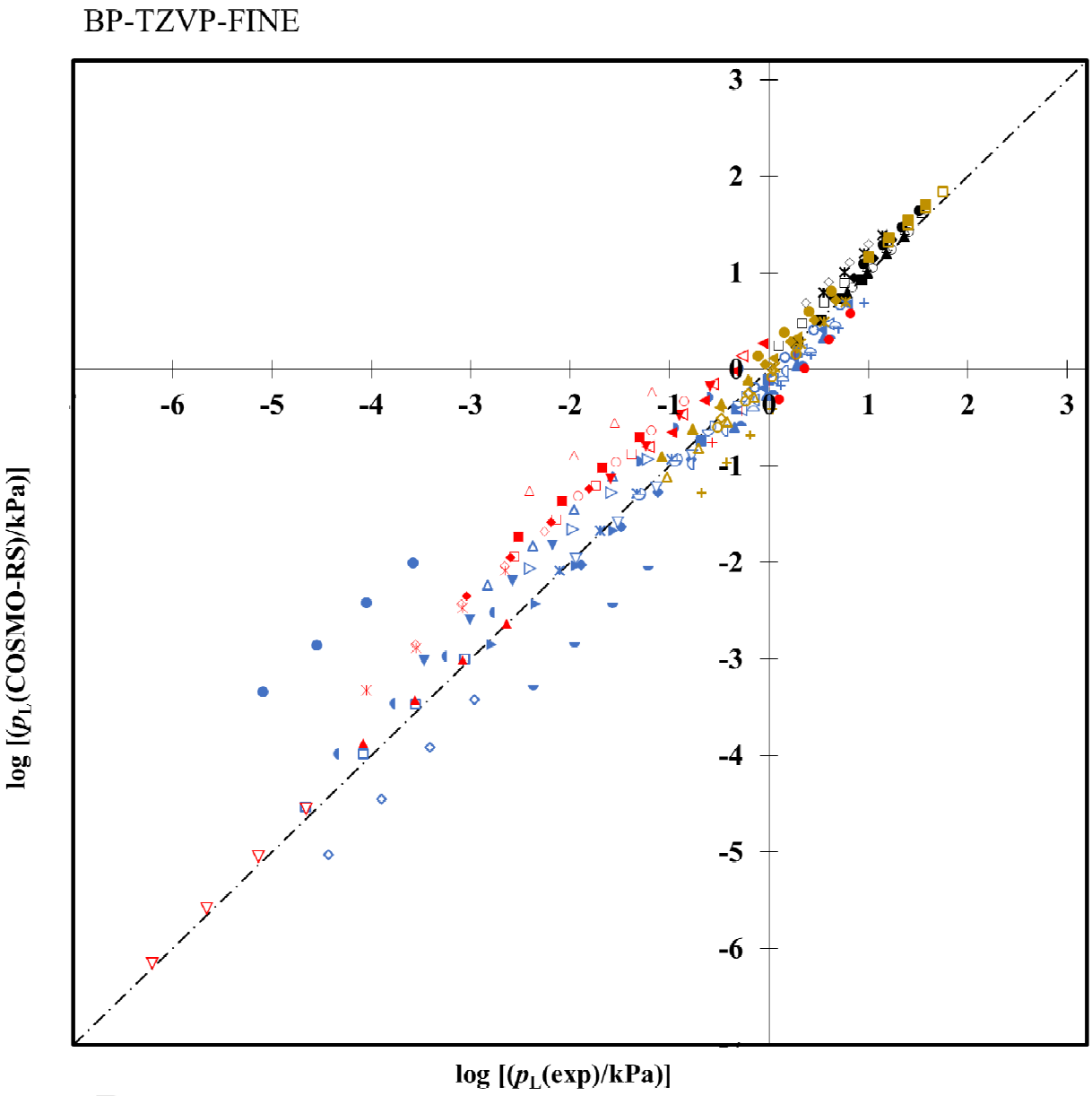

FIGURE 3. Logarithm of standard error of each estimate, at the BP-TZVP level of theory, full conformer sets.

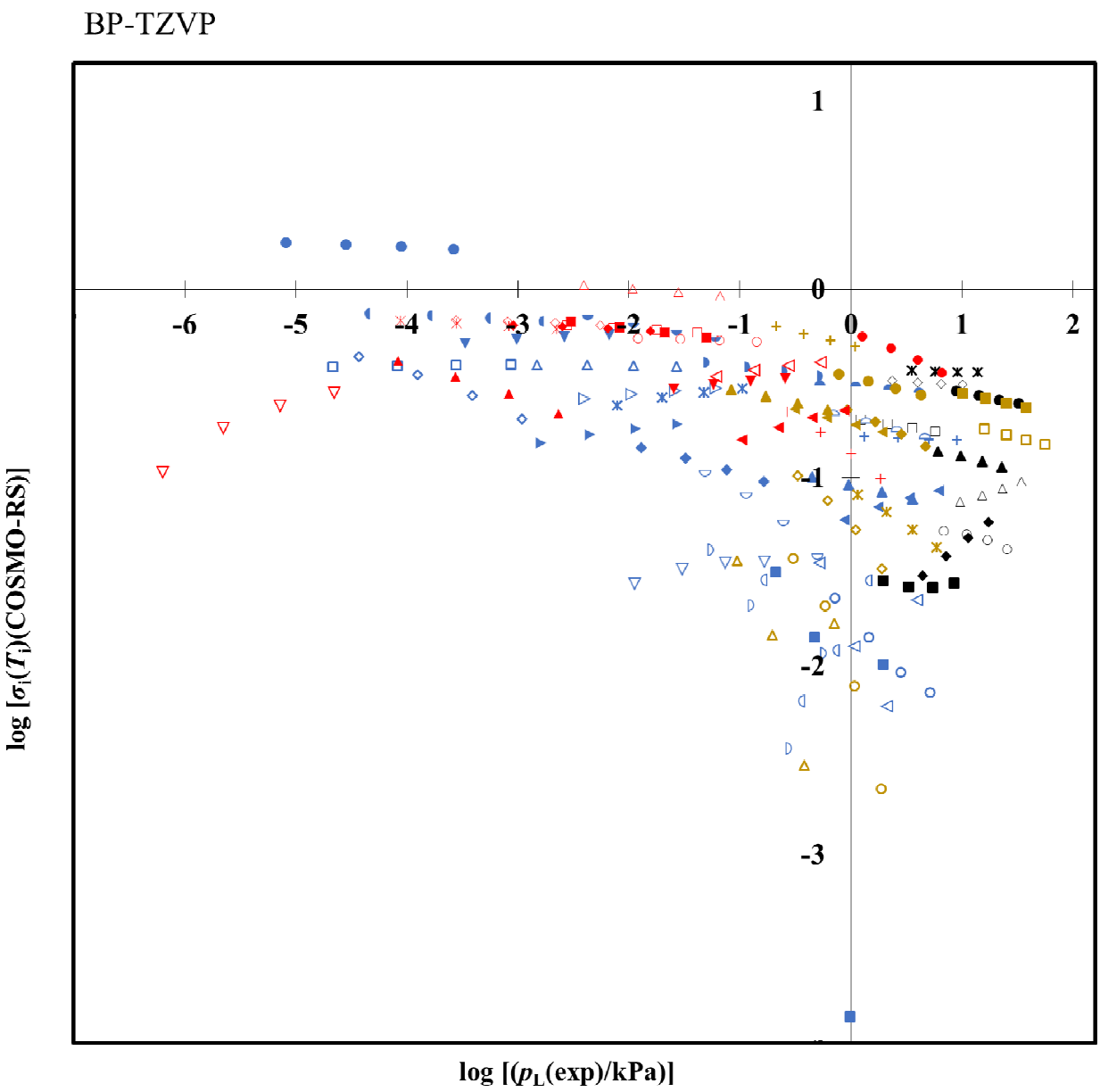

FIGURE 4. Logarithm of standard error of each estimate, at the BP-TZVPD-FINE level of theory, full conformer sets.

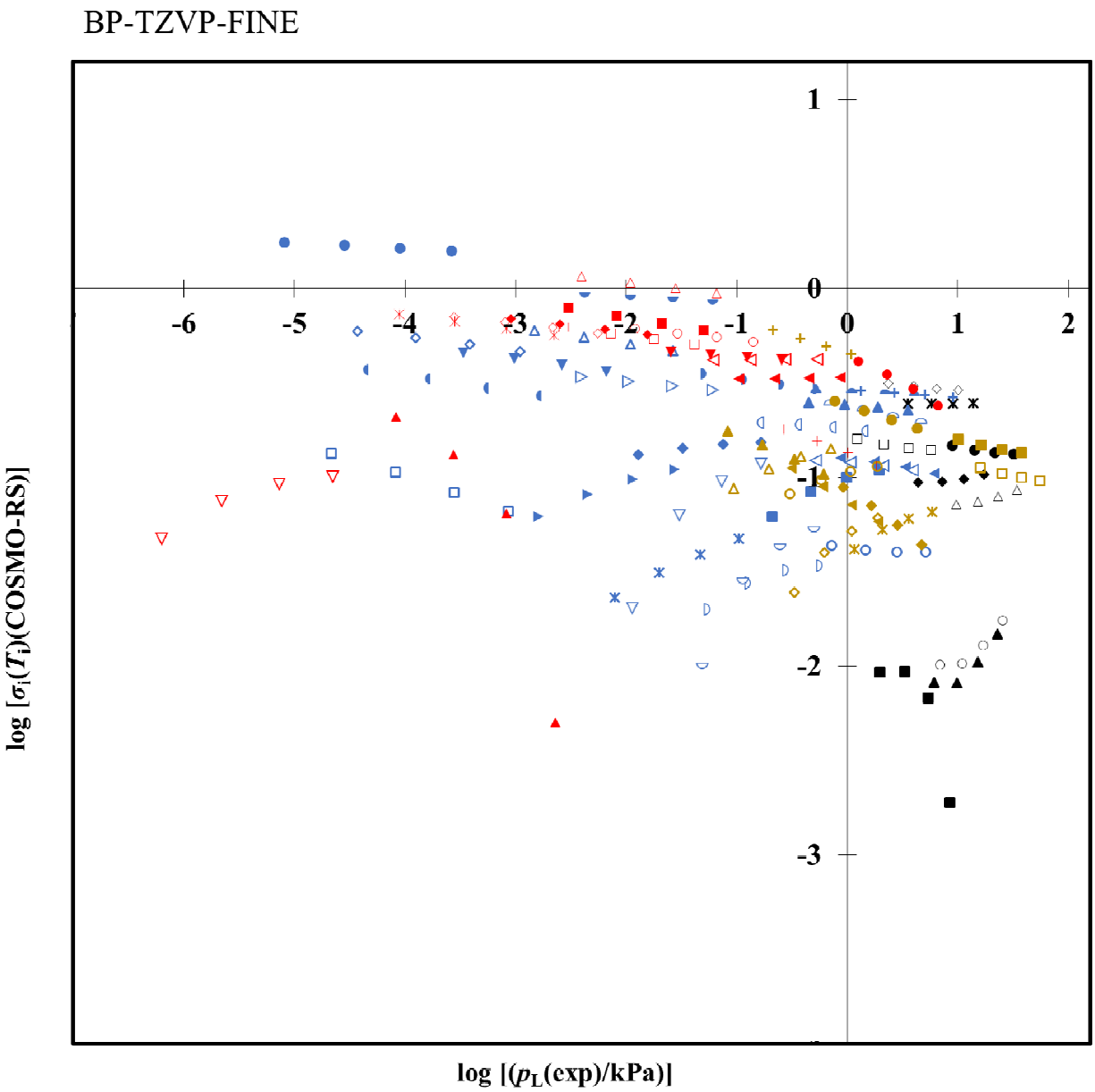

Highlights

- Review of available vapour pressures of oxygenates as used in (UNIFAC- p_L^o .1) with TDE
- Vapour pressure estimation with COSMO-RS on compounds with reliable experimental data
- Evaluation of COSMO-RS prediction behaviour on title compounds